BIOCHEMISTRY
including biophysical chemistry & molecular biology

Article

pubs.acs.org/biochemistry

Formal Reduction Potential of 3,5-Difluorotyrosine in a Structured Protein: Insight into Multistep Radical Transfer

Kanchana R. Ravichandran,[†] Li Liang,[‡] JoAnne Stubbe,[†] and Cecilia Tommos*[,‡]

[†]Department of Chemistry, Massachusetts Institute of Technology, 77 Massachusetts Avenue, Cambridge, Massachusetts 02139, United States

[‡]Graduate Group in Biochemistry and Molecular Biophysics and Department of Biochemistry and Biophysics, University of Pennsylvania, Philadelphia, Pennsylvania 19104, United States

Supporting Information

ABSTRACT: The reversible Y−O•/Y−OH redox properties of the α_3Y model protein allow access to the electrochemical and thermodynamic properties of 3,5-difluorotyrosine. The unnatural amino acid has been incorporated at position 32, the dedicated radical site in α_3Y, by *in vivo* nonsense codon suppression. Incorporation of 3,5-difluorotyrosine gives rise to very minor structural changes in the protein scaffold at pH values below the apparent pK (8.0 ± 0.1) of the unnatural residue. Square-wave voltammetry on α_3(3,5)F$_2$Y provides an $E^{o\prime}$(Y−O•/Y−OH) of 1026 ± 4 mV versus the normal hydrogen electrode (pH 5.70 ± 0.02) and shows that the fluoro substitutions lower the $E^{o\prime}$ by −30 ± 3 mV. These results illustrate the utility of combining the optimized α_3Y tyrosine radical system with *in vivo* nonsense codon suppression to obtain the formal reduction potential of an unnatural aromatic residue residing within a well-structured protein. It is further observed that the protein $E^{o\prime}$ values differ significantly from peak potentials derived from irreversible voltammograms of the corresponding aqueous species. This is notable because solution potentials have been the main thermodynamic data available for amino acid radicals. The findings in this paper are discussed relative to recent mechanistic studies of the multistep radical-transfer process in *Escherichia coli* ribonucleotide reductase site-specifically labeled with unnatural tyrosine residues.

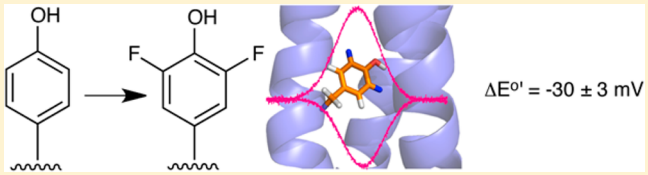

Tyrosine serves as a one-electron redox cofactor in catalytic and multistep electron-transfer reactions.[1−5] It has been challenging to obtain precise and accurate thermodynamic information for this high-potential protein redox species. Electrochemical characterization of the natural systems has not been feasible because of their size, complexity, and sensitivity to oxidative damage. Mechanistic studies of redox proteins employing tyrosine radical (Y•) cofactors must thus partly rely on model systems to provide insights into the thermodynamics involved. Reduction potentials (E values) of aqueous Y and various analogues have been obtained by pulse radiolysis and voltammetry methods.[6−11] Considerable uncertainty is associated with the reported values. This is in part due to varying experimental conditions, comparison of neutral and zwitterionic amino acids, and complicating issues such as solvent oxidation and the perturbation of solute−working electrode interactions. The most significant uncertainty, however, arises from the reactivity of the radical species themselves. Tyrosine radicals generated in solution will rapidly dimerize (~5 × 10^8 M^{-1} s^{-1})[12−16] and give rise to quasi-reversible or irreversible voltammograms.[17,18] Peak potentials (E_{peak}) derived from such data reflect the electrode process (electrode-driven oxidation−reduction of Y) as well as the thermodynamics and kinetics of the coupled side reactions (chemical reduction of Y•). The observed potentials may thus differ by tens even hundreds of millivolts from the formal (true) reduction potential ($E^{o\prime}$) of the Y redox system. Comparison between aqueous solution and protein Y redox chemistry is further complicated by the significant differences in the fundamental properties of these two media.[19,20]

The α_3X family of well-structured proteins was developed to address these concerns.[10,21] This model protein system yields thermodynamic information that is uncompromised by electrochemical irreversibility and radical side reactions.[22−24] The α_3X proteins are based on a common *de novo* designed three-helix bundle scaffold *GSR(1)*-**VKALEEKVKALEEKVKA**-*LGGGGR*-**IEELKKKX(32)EELKKKIEE**-*LGGGGE*-**VKKVEEEVK-KLEEEIKK**-*L(65)* (Sequence 1), where helical and loop regions are shown in bold and italic font, respectively. The N-terminal G and S residues of the 67-residue sequence form part of a thrombin cleavage site and are labeled as −2 and −1, respectively, to keep the amino acid numbering consistent between the chemically synthesized[10] and recombinantly expressed[25,26] α_3X proteins. The buried redox site (position 32 in the middle of the central helix) is occupied by a tryptophan (to form the α_3W protein), a tyrosine (α_3Y), or a cysteine (α_3C). C32 has been used to covalently attach phenol[24,26] and quinone[27] molecules to the protein scaffold. All of the α_3X proteins display very similar structural character-

Received: November 5, 2013
Published: November 14, 2013

   dx.doi.org/10.1021/bi401494f | *Biochemistry* 2013, 52, 8907−8915

istics. They are stable and well-structured from pH ∼4 to 10. Their single aromatic residue (W, Y, phenol, or quinone) gives rise to UV−vis, fluorescence, and nuclear magnetic resonance (NMR) spectra that are highly sensitive to the microenvironment of the redox site. Protein voltammetry has shown that the α_3X system displays unique electrochemical properties. The protein scaffold is redox inert to at least 1.3 V versus the normal hydrogen electrode (NHE).[22,24,26] The system becomes redox active when a W,[10] Y,[22,23] phenol,[24,26] or quinone[27] is introduced at position 32. Fully reversible voltammograms and $E^{\circ\prime}$ values have thus far been reported for the Y and phenol-containing α_3X proteins.[23,24]

In this study, we use the α_3X system in combination with the *in vivo* nonsense codon suppression method[28] and square-wave voltammetry (SWV)[17,29,30] to determine the $E^{\circ\prime}$ for a protein 3,5-difluorotyrosine (3,5-F_2Y) residue. We report $\Delta E^{\circ\prime}$ between 3,5-F_2Y and Y residues obtained under highly comparable experimental conditions. The results are compared to published solution potentials and discussed relative to recent mechanistic studies of *Escherichia coli* class Ia ribonucleotide reductase (RNR) site-specifically labeled with unnatural Y residues in an effort to understand the thermodynamic and kinetic landscape of the proton-coupled electron-transfer (PCET) pathway in this system.[28,31,32]

MATERIALS AND METHODS

Purification of Tyrosine Phenol Lyase (TPL). *E. coli* strain SVS370 harboring plasmid pTZTPL was obtained as a gift from R. Phillips (University of Georgia, Athens, GA). pTZTPL encodes TPL under a constitutive promoter, and the protein was expressed and purified[33,34] using a slightly modified procedure. The elution fractions from the octyl-Sepharose column were assayed using a coupled spectrophotometric assay in which a small volume of the fraction was added to an assay mixture containing 2 mM L-tyrosine, 5 mM β-mercaptoethanol, 50 μM pyridoxyl 5′-phosphate, 0.3 mg/mL lactate dehydrogenase (*Lactobacillus leichmannii* from Sigma-Aldrich), and 0.2 mM NADH in 50 mM potassium phosphate (pH 8.0). The reaction was monitored at 340 nm for the disappearance of NADH. Fractions containing considerable activity were pooled and concentrated in an Amicon ultrafiltration cell with a YM 10 membrane, and the protein was used with no additional purification steps. One unit of activity is defined as 1 μmol of product/min. A total of 62 units/g of cell paste was obtained, in excellent agreement with the previously reported yield.[33]

Enzymatic Synthesis of 3,5-Difluorotyrosine (3,5-F_2Y). TPL was used to enzymatically synthesize 3,5-F_2Y from 2,6-difluorophenol (the numbering of the aromatic ring changes as the OH carbon is position 1 in the phenol and position 4 in the amino acid). Briefly, a 1 or 2 L reaction mixture containing 10 mM 2,6-difluorophenol, 30 mM ammonium acetate (pH 8.0), 60 mM sodium pyruvate, 5 mM β-mercaptoethanol, 40 μM pyridoxyl 5′-phosphate, and 30 units of TPL at room temperature was stirred in the dark for a total of 4 days. The mixture was supplied with additional TPL, β-mercaptoethanol, and pyridoxyl 5′-phosphate every other day. Once the reaction was complete (as assessed by TLC), the mixture was worked up as described in ref 34. The yield is typically >85% for 3,5-F_2Y, and the final product was characterized by ^{1}H and ^{19}F NMR spectroscopy.[11,35]

Construction of α_3TAG32 by Site-Directed Mutagenesis. The amber stop codon (TAG) was introduced at position 32 of α_3Y using a modified pET32b-α_3Y plasmid[22,25] as a template, forward primer 5′-GGC GGC CGT ATT GAA GAA CTG AAA AAA AAA TAG GAA GAA CTG AAA AAA AAA ATT GAA GAA CTG GGC GGC GGC-3′, and reverse primer 5′-GCC GCC GCC CAG TTC TTC AAT TTT TTT TTT CAG TTC TTC CTA TTT TTT TTT CAG TTC TTC AAT ACG GCC GCC-3′. The mutation was performed using the Stratagene QuikChange kit and confirmed by sequencing at the Massachusetts Institute of Technology Biopolymers Laboratory.

Expression of α_3(3,5)F_2Y. pET32b-α_3TAG32 was cotransformed with a plasmid (pEVOL-F_nY-RS) encoding the fluorotyrosine tRNA and aminoacyl-tRNA synthetase (F_nY-RS) genes[28] into BL21(DE3) competent cells and grown on medium containing ampicillin (100 μg/mL) and chloramphenicol (35 μg/mL) at 37 °C. Unnatural amino acid concentration and protein expression were optimized on a small scale, resulting in the following protocol. LB precultures (40 mL) were started from single colonies, grown for ∼16 h, and used to inoculate (50-fold dilution) 1 L of 2xYT cultures containing 2.0 mM 3,5-F_2Y. Additions of 3,5-F_2Y were made from stock solutions freshly prepared in water, solubilized with NaOH, and sterile filtered. The expression of F_nY-RS was induced at an OD_{600} of 0.2−0.3 [L-arabinose, final concentration of 0.05% (w/v)]. The expression of α_3(3,5)F_2Y was induced at an OD_{600} of 0.5 (IPTG, final concentration of 1 mM). Growth was continued for an additional 4 h, and the cells were harvested by centrifugation (5000*g* for 15 min at 4 °C). Protein expression was monitored by sodium dodecyl sulfate−polyacrylamide gel electrophoresis (SDS−PAGE). No toxicity due to the unnatural amino acid was observed. Typical yields of 0.5 g of cell paste/100 mL and 2.5 g of cell paste/L of medium were obtained for the 0.1 and 1 L cultures, respectively.

Purification of α_3(3,5)F_2Y. Cell paste (∼5−10 g) was resuspended (5 mL/g paste) in buffer A [20 mM Tris-HCl, 500 mM NaCl, and 5 mM imidazole (pH 7.9)], treated with lysozyme (300 μg/mL, 30 min, 30 °C), and lysed by sonication. The lysate was clarified by centrifugation (12000*g* for 20 min at 4 °C) and passed over a nickel column [10 mL of His·bind resin (EMD Millipore)] that had been equilibrated with buffer A, and the thioredoxin fusions eluted with a linear gradient from 0 to 40% buffer B [20 mM Tris-HCl, 500 mM NaCl, and 1 M imidazole (pH 7.9)] over 40 min (flow rate of 1.5 mL/min). Fractions containing the thioredoxin fusions were identified by SDS−PAGE. Thrombin (T6634, Sigma-Aldrich) was added to the pooled fusion protein fractions [thrombin:-protein ratio of 1:2000 (w/w)] and the resulting mixture dialyzed against 20 mM Tris-HCl, 500 mM NaCl, and 2.5 mM $CaCl_2$ (pH 8.0) at room temperature for >16 h. The thrombin digestion produces three major products: His-tagged thioredoxin, the truncated α_3(residue 1−31) peptide (3579 Da), and the full-length α_3(3,5)F_2Y protein (7557 Da). A major fraction of the truncated α_3(residue 1−31) product was removed during the overnight dialysis step (Spectra/Por tubing, molecular mass cutoff of 3500 Da). The digestion/dialysis mixture (∼30 mL) was passed over a nickel column (10 mL of His·bind resin equilibrated with buffer A) to remove the His-tagged thioredoxin and any remaining undigested fusion products. α_3(3,5)F_2Y (sample injection volume of 5−10 mL) was isolated by reversed-phase high-performance liquid chromatography (HPLC) [218TP C18 column, particle size of 10 μm, column size of 10 mm × 250 mm (Grace/VYDAC)] using a linear water/acetonitrile/0.1% (w/v) trifluoroacetic acid gradient (30 to 60% acetonitrile over 45 min, flow rate of 5 mL/min) and

dx.doi.org/10.1021/bi401494f | *Biochemistry* 2013, 52, 8907−8915

stored as lyophilized powder. The protein purification steps were monitored by SDS−PAGE. The purity was evaluated by reversed-phase HPLC [218TP C18 column, particle size of 5 μm, column size of 4.6 mm × 250 mm (Grace/VYDAC)] using a linear water/acetonitrile/0.1% (w/v) trifluoroacetic acid gradient (20 to 70% acetonitrile over 50 min, flow rate of 1 mL/min). Molecular masses were verified by matrix-assisted laser desorption ionization time-of-flight (MALDI-TOF) mass spectrometry using a Bruker Microflex 3.1 instrument. An average yield of ∼3 mg of pure $\alpha_3(3,5)F_2Y$/L of culture was observed.

Absorption Spectroscopy. Absorption spectra were recorded on a Varian Cary 50 Bio UV−vis spectrometer at room temperature. Protein concentrations were determined by the Bradford protein assay (Bio-Rad) with standard curves prepared using either bovine serum albumin (for thioredoxin fusion samples) or α_3W[10] [for α_3Y and $\alpha_3(3,5)F_2Y$ protein characterization samples]. An ε_{280} of 5690 M^{-1} cm^{-1} was used for α_3W[10,36,37] when the standard curves were prepared. The apparent tyrosinate/tyrosine pK_a (pK_{app}) of $(3,5)F_2Y_{32}$ was measured by dissolving lyophilized $\alpha_3(3,5)F_2Y$ in 3.0 mL of 20 mM sodium acetate, 20 mM potassium phosphate, and 20 mM sodium borate (APB buffer) (pH 12) to give an absorption of 0.2 at 277 nm (10 mm path). The protein stock solution was added to 20 mM APB buffer generating two samples with pH values of ∼5 and ∼12. The pH was preadjusted in the APB buffer samples to generate the final pH upon addition of the protein stock. The protein dilution was 2-fold providing a final 277 nm absorption of 0.1 (10 mm path, pH 12). Equal-volume (1.6 mL) titration was performed manually by removing a 100−400 μL portion from the cuvette containing the high-pH sample and then adding the same amount of low-pH sample per pH adjustment. The pK_{app} was obtained by fitting the pH-induced increase in the $(3,5)F_2Y_{32}$−O^- absorption to a single pK_a.

Circular Dichroism (CD) Spectroscopy. CD data were collected on an Aviv 202 CD spectrometer at 25 °C. The instrument was equipped with an automated titration system. For the α-helical measurements, CD spectra were collected from α_3W, α_3Y, and $\alpha_3(3,5)F_2Y$ dissolved in 20 mM sodium acetate (pH 5.6). Protein concentrations were determined by the Bradford assay and using α_3W as the standard. pH titrations were performed by dissolving lyophilized protein in 20 mM APB buffer (pH 4.8) to a 235 nm ellipticity of approximately −175 mdeg (10 mm path). The protein stock solution was added to 20 mM APB buffer generating two samples with pH values of ∼4 and ∼10. The pH was preadjusted in the APB buffer samples to generate the final pH upon addition of the protein stock. The protein dilution was 4-fold generating a final 222 nm ellipticity of approximately −150 mdeg (10 mm path, pH 4). Equal-volume (2.5 mL) titration was performed manually by removing a 40−1000 μL portion from the cuvette containing the low-pH sample and then adding the same amount of high-pH sample per pH adjustment. Protein stability measurements were conducted by dissolving lyophilized protein in 20 mM sodium acetate and 20 mM potassium phosphate (AP buffer) (pH 5.0 or 5.5) to a 230 nm ellipticity of −75 to −140 mdeg (1 mm path). The protein stock solution was added to 20 mM AP buffer containing 0 and 9.5 M urea. The pH was 5.0 or 5.5 in the protein/AP buffer or protein/AP buffer/urea solution, respectively. The protein dilution was 18-fold generating a final 222 nm ellipticity in the range of −110 to −210 mdeg (10 mm path) at 0 M denaturant. The urea denaturation experiments were performed by automated equal-volume (2.0 mL) titration controlled by the Aviv software. Global stability values were determined by fitting the denaturation curves as described in ref 38.

Square-Wave Voltammetry (SWV). Voltammetry measurements[17,29,30] were performed using an Autolab PGSTAT12 potentiostat equipped with a temperature-controlled, Faraday cage-protected three-electrode microcell (Princeton Applied Research). The Ag/AgCl reference electrode and the platinum wire counter electrode (Advanced Measurements Inc.) were stored dry and prepared by filling the former with a 3 M KCl/saturated AgCl solution and the latter with sample buffer. All measurements were taken using a 3 mm diameter pyrolytic graphite edge (PGE) working electrode (Bio-Logic). The electrode surface was activated between measurements by manually polishing its surface for 60 s in a 1.0 μm diamond/water slurry on a diamond polishing pad (Bio-Logic) followed by 60 s in a 0.05 μm alumina/water slurry on a microcloth pad (Bioanalytical systems Inc.). The electrode was rinsed with an excess of methanol followed by Milli-Q water directed against the surface of the electrode. Measurements were performed immediately following the polishing procedures. The solution resistance was compensated for by using the positive feedback *iR* compensation function of the Autolab system. Potentials are given versus the NHE. All samples were prepared from ultrapure chemicals and the measurements performed under an argon atmosphere. Preparation of the voltammetry protein samples is described in the main text. Protein concentration series were obtained by stepwise dilution of the protein samples in the electrochemical cell while the sample volume was kept constant at 2.5 mL. The pH was monitored directly in the electrochemical cell using a pH microelectrode (Microelectrodes Inc.) connected to a SevenMulti pH meter (Mettler Toledo). The pH electrode was disconnected from the pH meter during the active measurements to prevent the risk of introducing electric noise. Data processing and analyses were performed using the Autolab GPES software and PeakFit (Systat Software Inc.).

RESULTS

$\alpha_3(3,5)F_2Y$ Expression and Purification. 3,5-Difluorotyrosine was synthesized enzymatically[33,34] as described in Materials and Methods. The amber stop codon (TAG) was introduced in place of the codon for residue 32 (Sequence 1) in a modified pET32b plasmid used for expression of the α_3X proteins.[22,25] The α_3TAG variant was co-expressed with an evolved polyspecific fluorotyrosine aminoacyl-tRNA synthetase[28] in *E. coli* BL21(DE3) cells. Protein expression was initially evaluated in 100 mL growth cultures by SDS−PAGE and mass spectrometry. Optimal expression was observed with 2.0 mM 3,5-F_2Y in 2xYT medium (see Figure S1 of the Supporting Information). The growth cultures were scaled to 1 L to generate sufficient material for protein characterization and voltammetry studies. Protein expression and purification protocols are described in detail in Materials and Methods. The purity of the $\alpha_3(3,5)F_2Y$ preparations was evaluated by reversed-phase HPLC (Figure S2A of the Supporting Information), and the correct protein molecular mass was verified by mass spectrometry (Figure S2B of the Supporting Information). The average yield of pure $\alpha_3(3,5)F_2Y$ was ∼3 mg/L of culture, which represents a suppression efficiency of only ∼10%. Efforts to improve the suppression efficiency are in progress.

Table 1. Properties of Y, 3,5-F_2Y, α_3Y, and $\alpha_3(3,5)F_2Y$

system	λ_{max} (nm)/ε (M^{-1} cm^{-1})	pK_a [pK_{app}]	potential vs NHE (mV)[e]	ref
Y(Ac/NH_2)[a]	275/1400 (Y−OH)	10	E_{peak}, 830 (pH 7.0)	31
	293/2420 ($Y-O^-$)			
3,5-F_2Y(Ac/NH_2)[a]	263/560 (Y−OH)	7.0 ± 0.2	E_{peak}, 770 (pH 7.0)	31
	275/1830 ($Y-O^-$)			
α_3Y	277/1500 (Y−OH, pH 5.4)	[11.3 ± 0.1]	$E^{o\prime}$, 1059 (pH 5.7)	10, 22, 23, this work
	294/2430 ($Y-O^-$, pH 13.4)		$E^{o\prime}$, 980 (pH 7.0)	
$\alpha_3(3,5)F_2Y$	~264/nd (Y−OH)[a]	[8.0 ± 0.1]	$E^{o\prime}$, 1026 (pH 5.7)	this work
	~277/nd ($Y-O^-$)[a]		$E^{o\prime}$, 952 (pH 7.0)[f]	
system	$[\Theta]_{222}$ ($\times 10^3$ deg cm^2 $dmol^{-1}$)	helix (%)[b]	ΔG (kcal mol^{-1})[g]	ref
α_3Y	−20.0 ± 0.8 (pH 5.6)	75 ± 3 (pH 5.6)[c]	−3.7 ± 0.1 (pH 5.0)	10, 22, this work
		74 ± 1 (pH 4.5−10)[d]	−3.9 ± 0.1 (pH 5.5)	
$\alpha_3(3,5)F_2Y$	−20.9 ± 0.6 (pH 5.6)	79 ± 2 (pH 5.6)[c]	−3.7 ± 0.1 (pH 5.0)	this work
			−3.7 ± 0.1 (pH 5.5)	

[a]Acetyl-tyrosinamide (Ac/NH_2). ε was not determined (nd). [b]Scaled relative to the $[\Theta]_{222}$ of α_3W (76 ± 1% α-helical, pH 4−10).[10,25] [c]Protein concentration determined by the Bradford assay. [d]Protein concentration determined by UV absorption.[10,22] [e]Anodic peak potentials from irreversible differential pulse voltammograms (E_{peak}).[10,11,31] The standard error in $E^{o\prime}$ is less than or equal to ±4 mV. [f]Extrapolated from the pH 5.7 value using a pH dependence of 59 mV/pH unit and a pK_{app} of 8.0. [g]From Figure S4 of the Supporting Information.

Protein Characterization. The aims of this study are to determine (i) the electrochemical reversibility of $\alpha_3(3,5)F_2Y$, (ii) the $E^{o\prime}$ of $(3,5)F_2Y_{32}$, and (iii) the $\Delta E^{o\prime}$ between $(3,5)F_2Y_{32}$ and Y_{32} when it is recorded under nearly identical conditions. Initially, we compared the structural properties of α_3Y and $\alpha_3(3,5)F_2Y$. α_3Y is highly helical and well-structured from pH 4.5 to 10.[10,22] The apparent $Y-O^-/Y-OH$ pK_a (pK_{app}) of Y_{32} is 11.3 ± 0.1 (Table 1). Exchanging Y_{32} with $(3,5)F_2Y_{32}$ was not expected to significantly perturb the protein scaffold[39,40] at pH values at which the buried phenol side chain is uncharged. Experiments were conducted to determine a suitable pH range for the SWV analysis, i.e., where $(3,5)F_2Y_{32}$ remains protonated and the structural properties of $\alpha_3(3,5)F_2Y$ closely resemble those of α_3Y.

Figure 1A displays absorption spectra of $\alpha_3(3,5)F_2Y$ recorded over a pH range from 5.7 (gray) to 10.4 (purple). The $(3,5)F_2Y_{32}-O^-/(3,5)F_2Y_{32}-OH$ transition titrates with a pK_{app} of 8.0 ± 0.1 (see Figure S3 of the Supporting Information for details). The protein environment increases the pK_{app} by ~1 unit relative to that of aqueous 3,5-F_2Y [pK_a = 7.0 ± 0.2 (Table 1)].[11,35] The weak and blue-shifted absorbance of aqueous 3,5-F_2Y−OH (ε_{263} = 560 M^{-1} cm^{-1}) relative to that of unmodified Y−OH [ε_{275} = 1400 M^{-1} cm^{-1} (Table 1)] was expected to translate into a rather poorly defined absorption spectrum of $\alpha_3(3,5)F_2Y$. The blue shift increases the level of spectral overlap between the absorption of the aromatic side chain and the large absorption of the protein backbone (λ_{max} = 190−220 nm), making $\alpha_3(3,5)F_2Y$ concentration measurements based on UV absorbance unreliable. Thus, the Bradford method was used to determine protein concentrations with standard curves prepared from α_3W. An ε_{277} of 1500 ± 80 M^{-1} cm^{-1} (pH 5.4) and an ε_{294} of 2430 ± 130 M^{-1} cm^{-1} (pH 13.4) were obtained for $Y_{32}-OH$ and $Y_{32}-O^-$ in α_3Y, respectively. The ε_{277} value is consistent with the average ε_{280} of 1490 M^{-1} cm^{-1} typically used for protein Y−OH residues[36,37] and close to the ε_{max} values of aqueous Y−OH (Table 1).[11] We conclude that the Bradford assay determines the α_3X protein concentration with good accuracy.

CD spectroscopy was used to measure the absolute α-helical content, the pH sensitivity of this parameter, and the global stability of $\alpha_3(3,5)F_2Y$ relative to α_3Y (Table 1). Figure 1B displays far-UV CD spectra of $\alpha_3(3,5)F_2Y$ (blue) and α_3Y (red) recorded at pH 5.6. The reference spectrum of the structurally characterized α_3W protein (green)[10,25] is also shown. The protein concentration in the CD samples was determined by the Bradford method. The CD spectral line shapes are essentially identical and display the characteristic 208/222 nm double minima of a predominantly α-helical protein. The 222 nm mean residue molar ellipticity ($[\Theta]_{222}$) reflects the α-helical content, which was estimated to be ~75−80% for $\alpha_3(3,5)F_2Y$ and α_3Y at pH 5.6 (Table 1). This translates into 50 ± 1 residues with helical ψ and ϕ backbone angles in $\alpha_3(3,5)F_2Y$ and α_3Y. This degree of helicity has consistently been observed for structurally characterized α_3X proteins [Protein Data Bank (PDB) entry 1LQ7[25] for α_3W and PDB entry 2LXY[24] for 2-mercaptophenol-α_3C]. Figure 1C displays $[\Theta]_{222}$ and the corresponding percent helix of $\alpha_3(3,5)F_2Y$ as a function of pH. The α-helical content of $\alpha_3(3,5)F_2Y$ decreases by only 2% from pH 4.7 to 6.7 and by 6% from pH 6.7 to 10. These small pH-induced changes in helical content are likely to be driven by the deprotonation of $(3,5)F_2Y_{32}$. The global stability of $\alpha_3(3,5)F_2Y$ and α_3Y was thus compared at acidic pH values >2 pH units below the pK_{app} of $(3,5)F_2Y_{32}$ (Figure S4 of the Supporting Information). The stability of the two proteins was found to be identical at pH 5.0 and to differ by only 0.2 kcal mol^{-1} at pH 5.5 (Table 1). The SWV analysis described below was conducted at low pH (5.6 ± 0.1), where the structural properties of $\alpha_3(3,5)F_2Y$ and α_3Y are very similar and their phenols are protonated.

Preparation of SWV Samples. The protein concentration is a key parameter to control when investigating the protein−working electrode interactions and optimizing the Faradaic response.[23,24] The high α-helical content of $\alpha_3(3,5)F_2Y$ makes CD spectroscopy a precise method for determining the protein concentration in a highly reproducible manner. Voltammetry samples were thus prepared by dissolving lyophilized protein in buffer until an appropriate θ_{222} was reached, and the protein concentration was calculated from the determined $[\Theta]_{222}$ value (see the legend of Figure 1). The supporting electrolyte, KCl, was added to the samples after the CD measurements to avoid UV absorption of the chloride ion.

SWV Analysis of $\alpha_3(3,5)F_2Y$. SWV voltammetry was conducted using a PGE working electrode. In SWV, the base potential (E_{step}) is changed incrementally in a series of forward

dx.doi.org/10.1021/bi401494f | Biochemistry 2013, 52, 8907−8915

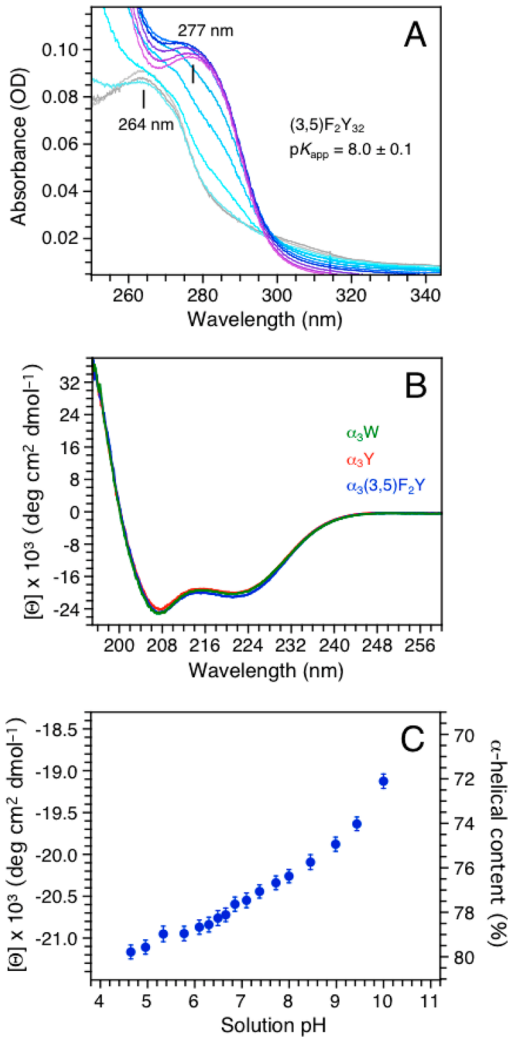

Figure 1. (A) pH titration of $\alpha_3(3,5)F_2Y$ monitored by UV−vis absorption spectroscopy. Spectra were recorded at pH 5.72 (gray), 6.38, 6.84, 7.49, 8.06, 8.53, 8.96, 9.31, 9.59, 10.02, and 10.42 (purple). (B) Far-UV CD spectra of $\alpha_3(3,5)F_2Y$ (blue), α_3Y (red), and α_3W (green) in 20 mM sodium acetate (pH 5.62 ± 0.01). The single aromatic residue in each protein is fully protonated at this pH. The CD spectra are displayed in units of mean residue molar ellipticity ($[\Theta]$) obtained from the equation $[\Theta] = \theta_{obs}[10^6/(Cln)]$, where θ_{obs} is the observed ellipticity in millidegrees (spectrometer raw signal), C the protein concentration in micromolar, l the cuvette path length in millimeters, and n the number of amino acid residues (65). $[\Theta]_{222}$ equals $(-20.9 \pm 0.6) \times 10^3$ deg cm^2 dmol^{-1} at pH 5.6 for $\alpha_3(3,5)F_2Y$ (Table 1). (C) Changes in the mean residue molar ellipticity ($[\Theta]$) and the corresponding level of α-helical content of $\alpha_3(3,5)F_2Y$ between pH 4.7 and 10.

and reverse pulses.[17,29,30] The pulse height and length are set by the SW amplitude (E_{SW}) and frequency (f), respectively. The current is sampled at the end of each alternating pulse and traced out as a function of E_{step}. The pulse train generates a forward voltammogram (I_{for}), a reverse voltammogram (I_{rev}), and a net voltammogram ($I_{net} = I_{for} - I_{rev}$). Previous studies using the PGE electrode have shown that ~20−100 μM α_3X in 20 mM APB buffer and 60−140 mM KCl yields Y and phenol voltammograms with optimal signal-to-noise ratios at both acidic (5.5) and alkaline (8.5) pH.[23,24] Under these conditions, the system is governed by diffusion-controlled kinetics, the protein does not unfold on the electrode surface, and the observed potential is independent of functional groups present at the electrode surface. The $\alpha_3(3,5)F_2Y$ SWV measurements were consequently conducted using 20 mM APB and 75 mM KCl. Overall, $\alpha_3(3,5)F_2Y$ displays electrochemical properties very similar to those of α_3Y.[23] The Faradaic response is consistent with diffusion-controlled kinetics (Figure S5 of the Supporting Information) and benign $\alpha_3(3,5)F_2Y$−working electrode interactions (Figure 2A,B). Figure 2C shows the change in the peak potential of the forward (I_{for}), reverse (I_{rev}), and net (I_{net}) currents as a function of the SW frequency. Background-corrected voltammograms from this series of data are shown in Figure 2D−F. E_{for}, E_{rev}, and E_{net} level off and come together as the SW frequency increases. This is consistent with a redox system that is shifting from the upper quasi-reversible region toward the fully reversible region as the SW frequency increases.[29,30] An E_{net} of 1026 ± 3 mV, an E_{for} of 1021 ± 3 mV, and an E_{rev} of 1032 ± 2 mV are observed for the 270−540 Hz range at pH 5.70 ± 0.02. The observed frequency insensitivity and small separation in peak maxima mean that E_{net} closely approximates $E^{\circ\prime}$ (i.e., within a few millivolts).[23,24,30] With a pK_{app} of 8.0, we calculate $E^{\circ\prime}$(pH 7.0) to be 952 mV (Table 1). Comparing these results with the earlier reported α_3Y SWV study[23] provides a $\Delta E^{\circ\prime}$ between Y_{32} and $(3,5)F_2Y_{32}$ of −28 to −33 mV. This result was reproduced in a control experiment in which $\alpha_3(3,5)F_2Y$ and α_3Y SW voltammograms were collected under identical experimental conditions, using the same electrode setup (Figure 3; $\Delta E_{net} = -30 \pm 3$ mV). We conclude that $E^{\circ\prime}$ of the Y32−O$^\bullet$/Y32−OH redox pair is lowered by 30 ± 3 mV upon fluoro substitution at ring positions 3 and 5 (carbon atoms next to the phenol oxygen). We further note that the difference between the E_{peak} of aqueous Y and the $E^{\circ\prime}$ of α_3Y is −150 mV, with the protein being the more oxidizing system (Table 1).

DISCUSSION

Measuring Tyrosine Reduction Potentials. There are three basic properties associated with tyrosine that make electrochemical characterization a major challenge. The measurements must be taken under highly oxidizing conditions (~+1.0 ± 0.3 V vs NHE); the Y$^\bullet$ state is reactive,[12−16] and both the reduced (ε_{280} = 1490 M^{-1} cm^{-1})[36,37] and oxidized (ε_{408} = 2750 M^{-1} cm^{-1})[41] states have weak extinction coefficients. The combination of these three properties rule out redox titration as a viable method for studying the thermodynamics of Y redox cofactors. This is a significant problem because redox titration, using either chemical titrants and a redox cuvette or a potentiostat-controlled spectroelectrochemical cell, is the most common approach to measuring reduction potentials of protein redox cofactors. The two former properties also make voltammetry a challenge. Measurements performed in the +1.0 V range will generate background currents arising from the working electrode and from the water solvent itself. These background currents will compromise data analysis unless the Faradaic current reflecting the Y redox cofactor is prominent. Moreover, uncontrolled oxidation of surface residues and general oxidative damage to the host protein are likely events. In addition to these concerns are the inherent issues associated with protein voltammetry, i.e., to identify conditions for which the folded protein exhibits direct and reversible electron transfer between the working electrode and the redox site of interest.[42−44] These are the main reasons that a direct voltammetry approach on a complex radical enzyme such as *E. coli* RNR is not practical or even possible.

dx.doi.org/10.1021/bi401494f | *Biochemistry* 2013, 52, 8907−8915

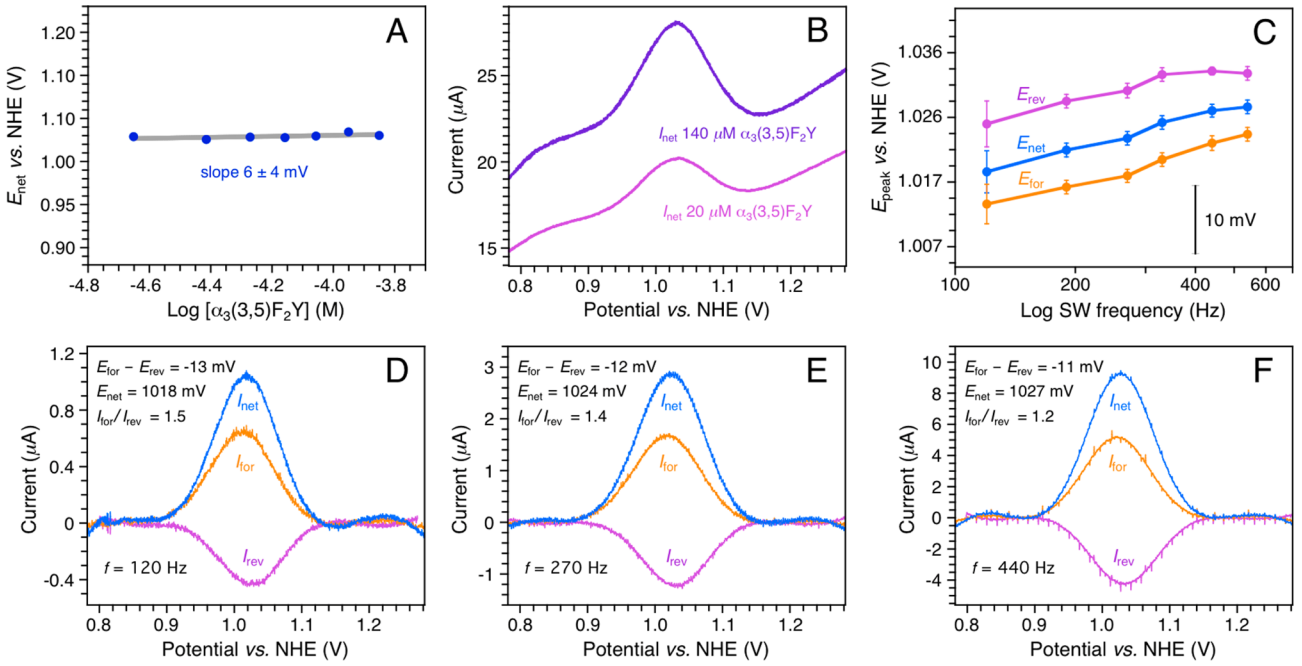

Figure 2. SWV analysis of the Y−O•/Y−OH redox system in $\alpha_3(3,5)F_2Y$. (A) E_{net}(270 Hz) as a function of [$\alpha_3(3,5)F_2Y$] at pH 5.53 ± 0.11. E_{net} is independent of the protein concentration, which is consistent with benign protein−working electrode interactions. (B) Representative net voltammograms (I_{net}) collected at the upper (140 μM, purple) and lower (20 μM, magenta) limits of the series of $\alpha_3(3,5)F_2Y$ concentrations shown in panel A. The Faradaic response is optimal in this protein concentration range. (C) Peak potential of the forward (E_{for}), reverse (E_{rev}), and net (E_{net}) $\alpha_3(3,5)F_2Y$ voltammograms as a function of SW frequency (f) at pH 5.70 ± 0.02. (D−F) Background-corrected voltammograms from the series of data shown in panel C. SWV settings: 20 mM APB, 75 mM KCl, PGE working electrode, temperature of 25 °C, step potential of 0.15 mV, and SW pulse amplitude of 25 mV.

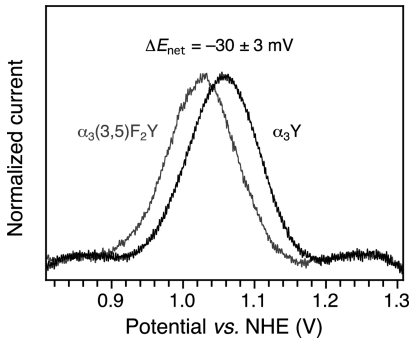

Figure 3. I_{net} of $\alpha_3(3,5)F_2Y$ (gray) and α_3Y (black) recorded under identical experimental conditions. SWV settings: 20 mM APB, 75 mM KCl, pH 5.62 ± 0.02, PGE working electrode, temperature of 25 °C, step potential of 0.15 mV, SW frequency of 190 Hz, and SW pulse amplitude of 25 mV.

The α_3X system was developed to address these experimental barriers and allow rigorous electrochemical characterization of aromatic amino acids buried within a structured protein. In three recent studies,[22−24] we have demonstrated that pulsed voltammetry methods (differential pulse voltammetry and SWV) generate high-quality reversible Y and phenol protein voltammograms. Control studies have shown that the characteristics of the α_3X voltammograms are highly reproducible and that they uniquely reflect the aromatic residue at position 32 and its local environment. The more commonly used method of cyclic voltammetry[17] generates a poor Faradaic response from the α_3X proteins,[22] and this method was deemed too insensitive for this system. We note that the potential range probed in this study is very oxidizing for a protein system with measured E_{net} values well above +1.0 V. The high quality of the presented voltammograms is the result of combining the sensitivity provided by the pulsed SWV method (caused by effective elimination of capacitative background currents) with carefully optimized protein−PGE working electrode conditions. The latter include electrode polishing procedures (described in Materials and Methods), the sample composition (optimized for the α_3X/PGE),[23,24] and the protein concentration (Figure 2A). Importantly, the electrochemical reversibility observed for the α_3X proteins reflects the long half-times (more than hundreds of milliseconds) of the radicals generated in this system.[23,24] Thus, the protein environment efficiently blocks the deleterious Y• side reactions that typically compromise electrochemical characterization of the solvated species.

In this study, the optimized α_3X radical system was combined with *in vivo* nonsense codon suppression[28] to measure the $E^{\circ\prime}$ of a protein 3,5-F_2Y residue. The use of unnatural amino acids to study protein electron-transfer (ET) and proton coupled electron-transfer (PCET) processes involving Y redox sites has emerged as an informative experimental approach.[31,45,46] The Y analogues provide a means for introducing major changes in the pK_a of the reduced state and in the $E^{\circ\prime}$ values of the Y−O•/Y−OH and Y−O•/Y−O$^-$ redox couples. The pK_a of the oxidized state (−2 for aqueous Y−OH•$^+$)[47] is predicted to be nonaccessible within the structural and catalytic pH ranges of proteins. Residue 32 resides in a structured, solvent-protected, and low-dielectric site typical of natural Y redox cofactors. The α_3X radical system will be used to generate a consistent set of $\Delta E^{\circ\prime}$ values to provide a guide for interpreting mutation-induced changes in the free energy profile of native ET/PCET chains involving aromatic amino acid redox site(s). The availability of protein $\Delta E^{\circ\prime}$ values removes the uncertainty

dx.doi.org/10.1021/bi401494f | *Biochemistry* 2013, 52, 8907−8915

associated with using solution potentials to interpret protein redox events. Table 1 shows that there are considerable differences in protein potentials obtained under reversible conditions relative to solution potentials obtained under irreversible conditions. We find a difference between $\Delta E^{\circ\prime}$ (protein Y_{32} and 3,5-F_2Y_{32}, −30 ± 3 mV) and ΔE_{peak} (aqueous Y and 3,5-F_2Y, −60 mV) of 30 mV (Table 1). This difference most certainly arises from the irreversible characteristics of the small molecule measurements. We also found that the absolute values of $E^{\circ\prime}$ (protein Y_{32} and 3,5-F_2Y_{32}) versus E_{peak} (aqueous Y and 3,5-F_2Y) are rather large (−150 to −180 mV). This observation suggests that the influence of the protein matrix on the absolute potentials of radical cofactors may be substantial. We conclude that site-specific incorporation of an unnatural amino acid into the electrochemically reversible α_3X redox system is a feasible and informative approach. It will be expanded to include other Y analogues in future studies, as described in more detail below.

Using the α_3X System as a Guide To Interpret Mechanistic Studies of *E. coli* RNR. RNRs catalyze the formation of deoxynucleotides (dNDPs) from their corresponding nucleotides.[1,31] *E. coli* class Ia RNR is composed of two homodimeric subunits, α2 and β2. A stable diferric-$Y_{122}^{\bullet}$ cofactor in β2 generates a transient cysteine radical ($C_{439}^{\bullet}$) in the active site of α2 located 35 Å away. The reversible long-range radical-transfer process, triggered by binding of the substrate and effector to α2, is proposed to involve multiple PCET steps via a conserved pathway ($Y_{122} \Leftrightarrow [W_{48}] \Leftrightarrow Y_{356}$ in β2 to $Y_{731} \Leftrightarrow Y_{730} \Leftrightarrow C_{439}$ in α2).[31] We have recently described the site-specific insertion of 3-nitrotyrosine (NO_2Y) in place of Y_{122} in β2.[48] The diferric $NO_2Y_{122}^{\bullet}$ cofactor was generated, and studies with α2, substrate (CDP), and effector (ATP) allowed the first observation of a transient, kinetically competent $Y^{\bullet}$ on pathway by electron paramagnetic resonance (EPR) spectroscopy.[48] Pulsed electron−electron double resonance (PELDOR) spectroscopy was used to establish the primary location of the new radical as $Y_{356}^{\bullet}$-β2 and suggested the formation of a small percentage of radical at either Y_{731} or Y_{730} in α2. To probe this further, the reaction of diferric $NO_2Y_{122}^{\bullet}$-β2 with (3,5)F_2Y_{731}-α2 [or (3,5)F_2Y_{730}-α2], CDP, and ATP was performed. Analysis of the reactions by X-band EPR spectroscopy demonstrated an equilibrium between $Y_{356}^{\bullet}$ in β2 and (3,5)$F_2Y_{731}^{\bullet}$ or (3,5)$F_2Y_{730}^{\bullet}$ in α2 with 85−90% of the spin localized at Y_{356} and 15−10% distributed over F_2Y_{731}/F_2Y_{730}.[32] Extrapolating the equilibrium observed with 3,5-F_2Y to Y, the native pathway residue, requires a knowledge of $E^{\circ\prime}$ values for 3,5-F_2Y and Y. To date, only solution E_{peak} values derived from irreversible voltammograms have been available for the fluorotyrosines.[11,31] The SWV measurements performed on α_3Y and α_3(3,5)F_2Y provide the first $E^{\circ\prime}$ values representing the radical species in a well-defined protein environment. The small $\Delta E^{\circ\prime}$ of −30 ± 3 mV between Y_{32} and 3,5-F_2Y_{32} suggests that a thermodynamic landscape, formed by three transient tyrosyl radicals (Y_{356}, Y_{731}, and Y_{730}) of similar energies with one being most prevalent, is a reasonable depiction of nature's design within this part of the pathway.

Future Perspectives. We have shown that formal reduction potentials representing a reversible Y−O$^{\bullet}$/Y−OH redox system can be obtained for α_3Y[23] and α_3(3,5)F_2Y (this work). Future studies will involve the incorporation of other modified amino acids at position 32 in the α_3X scaffold to yield a consistent set of $E^{\circ\prime}$ values from Y and modified Y residues. Determining the $E^{\circ\prime}$ of 3-aminotyrosine (NH_2Y) and 2,3,5-trifluorotyrosine (2,3,5-F_3Y) incorporated into the α_3X protein is of particular interest. In the former case, studies with NH_2Y in place of Y_{356}, Y_{731}, and Y_{730} show an active pathway that can produce dNDPs.[49] This is an interesting observation because the solution potential of NH_2Y[9] suggests that this species may act as a radical sink shutting down the pathway, as observed in experiments with 3,4-dihydroxyphenylalanine (DOPA)-labeled Y_{356}-β2.[50] Obtaining a solid protein $\Delta E^{\circ\prime}$ value for NH_2Y_{32} versus Y_{32} would be valuable for interpreting the characteristics of the NH_2Y-labeled RNR systems (see ref 31 for more details). In the latter case, experiments to measure the thermodynamics between Y_{122} and Y_{356} in β2 are in progress. With that goal in mind, diferric $F_nY_{122}^{\bullet}$ (n = 2 or 3)-β2 species have been successfully generated, and the reactions of (3,5)$F_2Y_{122}^{\bullet}$-β2 and (2,3,5)$F_3Y_{122}^{\bullet}$-β2 with α2, CDP, and ATP have been analyzed by EPR spectroscopy.[28,31] These studies reveal that only (2,3,5)$F_3Y_{122}^{\bullet}$ is capable of generating a new pathway radical that is postulated to be $Y_{356}^{\bullet}$. Detailed investigations with F_nY-β2 species and wt-α2 (or Y_{731}F-α2) are ongoing to establish if there is an equilibrium between $Y_{356}^{\bullet}$ and F_nY_{122}. Thus, protein $E^{\circ\prime}$ values of (2,3,5)F_3Y and other F_nY residues relative to Y may also play an important role in defining the thermodynamic landscape within this part of the pathway. Finally, work to complement the α_3X protein $E^{\circ\prime}$ data series with α_3W potentials is also in progress. Tryptophan is an important protein redox cofactor observed in a number of enzymes (e.g., refs 51−53), proposed to participate in the *E. coli* RNR radical-transfer pathway,[54,55] and engineered to study multistep electron tunneling in *Pseudomonas aeruginosa* azurin.[56]

■ ASSOCIATED CONTENT

Supporting Information

Materials and Methods, α_3(3,5)F_2Y protein expression analysis (Figure S1), HPLC and MALDI-TOF evaluation of purified α_3(3,5)F_2Y (Figure S2), pK_{app} fitting analysis (Figure S3), chemical denaturation plots of α_3(3,5)F_2Y and α_3Y at pH 5.0 and 5.5 (Figure S4), and α_3(3,5)F_2Y I_{net} as a function of E_{SW} (Figure S5). This material is available free of charge via the Internet at http://pubs.acs.org.

■ AUTHOR INFORMATION

Corresponding Author

*Address: 905 Stellar-Chance Laboratories, Department of Biochemistry and Biophysics, University of Pennsylvania, 422 Curie Blvd., Philadelphia, PA 19104-6059. E-mail: tommos@mail.med.upenn.edu. Telephone: (215) 746-2444. Fax: (215) 573-7290.

Funding

Funding was provided by National Institutes of Health Grants GM079190 (C.T.) and GM29595 (J.S.).

Notes

The authors declare no competing financial interest.

■ ABBREVIATIONS

α2 and β2, subunits of *E. coli* RNR; α_3Y, α_3W, or α_3C, *de novo* proteins containing a single buried tyrosine, tryptophan, or cysteine, respectively; α_3X, generic designation for this protein family; α_3(3,5)F_2Y, α_3Y containing 3,5-difluorotyrosine; APB buffer, sodium acetate, potassium phosphate, sodium borate buffer; CDP, cytidine 5′-diphosphate; $E^{\circ\prime}$, formal reduction potential; E_{peak}, voltammetry peak potential; E_{for}, E_{rev}, and E_{net}, peak potentials of the forward, reverse, and net currents,

respectively, in SWV; E_{step}, staircase base potential in SWV; E_{SW}, square-wave pulse amplitude; EPR, electron paramagnetic resonance; ET, electron transfer; f, square-wave frequency; F_nY (n = 2 and 3), di- and trisubstituted fluorotyrosines, respectively; F_nY-RS, fluorotyrosine aminoacyl-tRNA synthetase; pK_{app}, apparent pK_a; I_{for}, I_{rev}, and I_{net}, forward, reverse, and net currents, respectively, in SWV; PCET, proton-coupled electron transfer; PGE, pyrolytic graphite edge; RNR, ribonucleotide reductase; SWV, square-wave voltammetry; TPL, tyrosine phenol lyase; $Y^{\bullet}$, tyrosine radical.

REFERENCES

(1) Stubbe, J., and van der Donk, W. A. (1998) Protein radicals in enzyme catalysis. *Chem. Rev. 98*, 705−762.

(2) Tommos, C., and Babcock, G. T. (2000) Proton and hydrogen currents in photosynthetic water oxidation. *Biochim. Biophys. Acta 1458*, 199−219.

(3) Pesavento, R. P., and van der Donk, W. A. (2001) Tyrosyl radical cofactors. *Adv. Protein Chem. 58*, 317−385.

(4) Hoganson, C. W., and Tommos, C. (2004) The function and characteristics of tyrosyl radical cofactors. *Biochim. Biophys. Acta 1655*, 116−122.

(5) Warren, J. J., Winkler, J. R., and Gray, H. B. (2012) Redox properties of tyrosine and related molecules. *FEBS Lett. 586*, 596−602.

(6) Harriman, A. (1987) Further comments on the redox potentials of tryptophan and tyrosine. *J. Phys. Chem. 91*, 6102−6104.

(7) DeFelippis, M. R., Murthy, C. P., Faraggi, M., and Klapper, M. H. (1989) Pulse radiolytic measurement of redox potentials: The tyrosine and tryptophan radicals. *Biochemistry 28*, 4847−4853.

(8) Lind, J., Shen, X., Eriksen, T. E., and Merényi, G. (1990) The one-electron reduction potential of 4-substituted phenoxyl radicals in water. *J. Am. Chem. Soc. 112*, 479−482.

(9) DeFelippis, M. R., Murthy, C. P., Broitman, F., Weinraub, D., Faraggi, M., and Klapper, M. H. (1991) Electrochemical properties of tyrosine phenoxy and tryptophan indolyl radicals in peptides and amino acid analogues. *J. Phys. Chem. 95*, 3416−3419.

(10) Tommos, C., Skalicky, J. J., Pilloud, D. L., Wand, A. J., and Dutton, P. L. (1999) De novo proteins as models of radical enzymes. *Biochemistry 38*, 9495−9507.

(11) Seyedsayamdost, M. R., Reece, S. Y., Nocera, D. G., and Stubbe, J. (2006) Mono-, di-, tri-, and tetra-substituted fluorotyrosines: New probes for enzymes that use tyrosyl radicals in catalysis. *J. Am. Chem. Soc. 128*, 1569−1579.

(12) Gross, A. J., and Sizer, I. W. (1959) The oxidation of tyramine, tyrosine, and related compounds by peroxide. *J. Biol. Chem. 234*, 1611−1614.

(13) Lehrer, S. S., and Fasman, G. D. (1967) Ultraviolet irradiation effects in poly-L-tyrosine and model compounds. Identification of bityrosine as a photoproduct. *Biochemistry 6*, 757−767.

(14) Boguta, G., and Dancewicz, A. M. (1981) Radiation-induced dimerization of tyrosine and glycyltyrosine in aqueous solutions. *Int. J. Radiat. Biol. 39*, 163−174.

(15) Karam, L. R., Dizdaroglu, M., and Simic, M. G. (1984) OH radical-induced products of tyrosine peptides. *Int. J. Radiat. Biol. 46*, 715−724.

(16) Hawkins, C. L., and Davies, M. J. (2001) Generation and propagation of radical reactions on proteins. *Biochim. Biophys. Acta 1504*, 93−109.

(17) Bard, A. J., and Faulkner, L. R. (2001) *Electrochemical methods: Fundamentals and applications*, 2nd ed., John Wiley & Sons, Inc., New York.

(18) Savéant, J. M. (2006) *Elements of molecular and biomolecular electrochemistry: An electrochemical approach to electron transfer chemistry*, John Wiley & Sons, Inc., New York.

(19) Warshel, A., Sharma, P. K., Kato, M., Xiang, Y., Liu, H., and Olsson, M. H. M. (2006) Electrostatic basis for enzyme catalysis. *Chem. Rev. 106*, 3210−3235.

(20) Chandler, D. (2005) Interfaces and the driving force of hydrophobic assembly. *Nature 437*, 640−647.

(21) Westerlund, K., Berry, B. W., Privett, H. K., and Tommos, C. (2005) Exploring amino-acid radical chemistry: Protein engineering and *de novo* design. *Biochim. Biophys. Acta 1707*, 103−116.

(22) Martínez-Rivera, M. C., Berry, B. W., Valentine, K. G., Westerlund, K., Hay, S., and Tommos, C. (2011) Electrochemical and structural properties of a protein system designed to generate tyrosine Pourbaix diagrams. *J. Am. Chem. Soc. 133*, 17786−17795.

(23) Berry, B. W., Martínez-Rivera, M. C., and Tommos, C. (2012) Reversible voltammograms and a Pourbaix diagram for a protein tyrosine radical. *Proc. Natl. Acad. Sci. U.S.A. 109*, 9739−9743.

(24) Tommos, C., Valentine, K. G., Martínez-Rivera, M. C., Liang, L., and Moorman, V. R. (2013) Reversible phenol oxidation and reduction in the structurally well-defined 2-mercaptophenol-α_3C protein. *Biochemistry 52*, 1409−1418.

(25) Dai, Q.-H., Tommos, C., Fuentes, E. J., Blomberg, M. R. A., Dutton, P. L., and Wand, A. J. (2002) Structure of a de novo designed model protein of radical enzymes. *J. Am. Chem. Soc. 124*, 10952−10953.

(26) Hay, S., Westerlund, K., and Tommos, C. (2005) Moving a phenol hydroxyl group from the surface to the interior of a protein: Effects on the phenol potential and pK_a. *Biochemistry 44*, 11891−11902.

(27) Hay, S., Westerlund, K., and Tommos, C. (2007) Redox characteristics of a de novo quinone protein. *J. Phys. Chem. B 111*, 3488−3495.

(28) Minnihan, E. C., Young, D. D., Schultz, P. G., and Stubbe, J. (2011) Incorporation of fluorotyrosines into ribonucleotide reductase using an evolved, polyspecific aminoacyl-tRNA synthetase. *J. Am. Chem. Soc. 133*, 15942−15945.

(29) Osteryoung, J., and O'Dea, J. J. (1986) Square-wave voltammetry. In *Electroanalytical Chemistry* (Bard, A. J., Ed.) Vol. 5, pp 209−308, Marcel Dekker, New York.

(30) Mirčeski, V., Komorsky-Lovrić, Š., and Lovrić, M. (2007) Square-wave voltammetry: Theory and applications. In *Monographs in Electrochemistry* (Scholz, F., Ed.) Springer-Verlag, Berlin.

(31) Minnihan, E. C., Nocera, D. G., and Stubbe, J. (2013) Reversible, long-range radical transfer in *E. coli* class 1a ribonucleotide reductase. *Acc. Chem. Res. 46*, 2524−2535.

(32) Yokoyama, K., Smith, A. A., Corzilius, B., Griffin, R. G., and Stubbe, J. (2011) Equilibration of tyrosyl radicals ($Y_{356}^{\bullet}$, $Y_{731}^{\bullet}$, $Y_{730}^{\bullet}$) in the radical propagation pathway of the *Escherichia coli* Class 1a ribonucleotide reductase. *J. Am. Chem. Soc. 133*, 18420−18432.

(33) Chen, H., Gollnick, P., and Phillips, R. S. (1995) Site-directed mutagenesis of His343 → Ala in *Citrobacter freundii* tyrosine phenol-lyase: Effects on the kinetic mechanism and rate-determining step. *Eur. J. Biochem. 229*, 540−549.

(34) Seyedsayamdost, M. R., Yee, C. S., and Stubbe, J. (2007) Site-specific incorporation of fluorotyrosines into the R2 subunit of *E. coli* ribonucleotide reductase by expressed protein ligation. *Nat. Protoc. 2*, 1225−1235.

(35) Kim, K., and Cole, P. A. (1998) Kinetic analysis of a protein tyrosine kinase reaction transition state in the forward and reverse directions. *J. Am. Chem. Soc. 120*, 6851−6858.

(36) Edelhoch, H. (1967) Spectroscopic determination of tryptophan and tyrosine in proteins. *Biochemistry 6*, 1948−1954.

(37) Pace, C. N., Vajdos, F., Fee, L., Grimsley, G., and Gray, T. (1995) How to measure and predict the molar absorption coefficient of a protein. *Protein Sci. 4*, 2411−2423.

(38) Santoro, M. M., and Bolen, D. W. (1988) Unfolding free energy changes determined by the linear extrapolation method. 1. Unfolding of phenylmethanesulfonyl α-chymotrypsin using different denaturants. *Biochemistry 27*, 8063−8068.

(39) Salwiczek, M., Nyakatura, E. K., Gerling, U. I. M., Ye, S., and Koksch, B. (2012) Fluorinated amino acids: Compatibility with native protein structures and effects on protein−protein interactions. *Chem. Soc. Rev. 41*, 2135−2171.

(40) Buer, B. C., and Marsh, E. N. G. (2012) Fluorine: A new element in protein design. *Protein Sci. 21*, 453−462.
(41) Feitelson, J., and Hayon, E. (1973) Electron ejection and electron capture by phenolic compounds. *J. Phys. Chem. 77*, 10−15.
(42) Rusling, J. F. (1998) Enzyme bioelectrochemistry in cast biomembrane-like films. *Acc. Chem. Res. 31*, 363−369.
(43) Armstrong, F. A., and Wilson, G. S. (2000) Recent developments in faradaic bioelectrochemistry. *Electrochim. Acta 45*, 2623−2645.
(44) Armstrong, F. A. (2005) Recent developments in dynamic electrochemical studies of adsorbed enzymes and their active sites. *Curr. Opin. Chem. Biol. 9*, 110−117.
(45) Rappaport, F., Boussac, A., Force, D. A., Peloquin, J., Brynda, M., Sugiura, M., Un, S., Britt, R. D., and Diner, B. A. (2009) Probing the coupling between proton and electron transfer in photosystem II core complexes containing a 3-fluorotyrosine. *J. Am. Chem. Soc. 131*, 4425−4433.
(46) Warren, J. J., Herrera, N., Hill, M. G., Winkler, J. R., and Gray, H. B. (2013) Electron flow through nitrotyrosine in *Pseudomonas aeruginosa* azurin. *J. Am. Chem. Soc. 135*, 11151−11158.
(47) Dixon, W. T., and Murphy, D. (1976) Determination of the acidity constants of some phenol radical cations by means of electron spin resonance. *J. Chem. Soc., Faraday Trans. II 72*, 1221−1230.
(48) Yokoyama, K., Uhlin, U., and Stubbe, J. (2010) A hot oxidant, 3-NO_2Y_{122} radical, unmasks conformational gating in ribonucleotide reductase. *J. Am. Chem. Soc. 132*, 15368−15379.
(49) Seyedsayamdost, M. R., Xie, J., Chan, C. T. Y., Schultz, P. G., and Stubbe, J. (2007) Site-specific insertion of 3-aminotyrosine in subunit α2 of *E. coli* ribonucleotide reductase: Direct evidence for involvement of Y_{730} and Y_{731} in radical propagation. *J. Am. Chem. Soc. 129*, 15060−15071.
(50) Seyedsayamdost, M. R., and Stubbe, J. (2006) Site-specific replacement of Y_{356} with 3,4-dihydroxyphenlalanine in the β2 subunit of *E. coli* ribonucleotide reductase. *J. Am. Chem. Soc. 128*, 2522−2523.
(51) Tsai, A.-L., and Kulmacz, R. J. (2010) Prostaglandine H synthesis: Resolved and unresolved mechanistic issues. *Arch. Biochem. Biophys. 493*, 103−124.
(52) Aubert, C., Vos, M. H., Mathis, P., Eker, A. P. M., and Brettel, K. (2000) Intraprotein radical transfer during photoactivation of DNA photolyase. *Nature 405*, 586−590.
(53) Tarboush, N. A., Jensen, L. M. R., Yukl, E. T., Geng, J., Liu, A., Wilmot, C. M., and Davidson, V. L. (2011) Mutagenesis of tryptophan 199 suggests that hopping is required for MauG-dependent tryptophan tryptophylquinone biosynthesis. *Proc. Natl. Acad. Sci. U.S.A. 108*, 16956−16961.
(54) Uhlin, U., and Eklund, H. (1994) Structure of ribonucleotide reductase protein R1. *Nature 370*, 533−539.
(55) Ekberg, M., Birgander, P., and Sjöberg, B.-M. (2003) In vivo assay for low-activity mutant forms of *Escherichia coli* ribonucleotide reductase. *J. Bacteriol. 185*, 1167−1173.
(56) Shih, C., Museth, A. K., Abrahamsson, M., Blanco-Rodriguez, A. M., Di Bilio, A. J., Sudhamsu, J., Crane, B. R., Ronayne, K. L., Towrie, M., Vlcek, A., Jr., Richards, J. H., Winkler, J. R., and Gray, H. B. (2008) Tryptophan-accelerated electron flow through proteins. *Science 320*, 1760−1762.